Automated Scan Plane Alignment for Robot-Based Planar Near-Field Antenna Measurements

R. Moch[1], MEMBER, AMTA, and Q. Ton[1], and P. Pelland[1], FELLOW, AMTA.
(1) NSI-MI Technologies AMETEK, Suwanee, Georgia, U.S.

***Abstract*—An automated scan plane alignment technique for robot-based planar near-field antenna measurements enables precise and efficient calibration of unknown and arbitrarily oriented antennas under test (AUTs). By integrating a high-resolution laser line profile sensor with a robotic arm, the system dynamically determines the AUT's position, orientation, and outline without requiring detailed prior knowledge. A real-time feedback loop guides the robot to adaptively align the scan plane based on measured surface profiles, taking into account tilts or non-ideal AUT placements. Edge detection and reference mark identification further enhance accuracy, allowing to precisely align the scan center with the AUT's geometric center. The method is validated using a reference metal plate and is particularly suited for spatially flat antennas or radomes. Beyond alignment, the same setup enables high-resolution optical inspection, capable of detecting fine surface details such as cracks, dents, or even the thickness of ink from printing. The approach significantly reduces setup time by eliminating manual alignment steps, and broadens the functionality of robot-based measurement systems by combining self-alignment and optical inspection into a single automated process.**

***Index Terms*—antenna measurements, calibration, measurement systems, near-field, robotic systems.**

I. Introduction

Robot-based positioners are an emerging technology in the domain of near-field antenna measurements, whether it concerns high-throughput production tests [1], radome measurements [2] or multi-purpose antenna measurement systems [3], [4]. They provide the required flexibility to support all conventional sampling geometries, including planar, cylindrical, spherical or even non-canonical measurements [5]. Beyond that, robot-based positioners also enable a streamlining of the alignment process which is for typical positioners often a manual and time-consuming task usually performed by the range operator. For these conventional positioners, certain degrees of freedom may be mechanically limited and, thus, eventual misalignments cannot be compensated at all. However, utilizing the robot's degrees of freedom, the alignment between the antenna under test (AUT) and the sampling geometry can be ensured. This includes situations in which the AUT itself cannot be re-aligned and, instead, the sampling grid is adjusted relative to the AUT or other mechanical reference points. To determine the correct alignment, either external sensors or electrical alignment methods can be used if the AUT is known. For the latter, approaches exist specifically for robot-based spherical near-field antenna measurements [6]. While these methods can be automated in principle, the large amount of necessary measurements takes a considerable amount of time. Other more generic approaches based on external sensors, for example laser trackers [7], allow the system to determine the alignment without requiring a known AUT. However, these are more commonly used for one-time alignment of a measurement range due to the complexity and cost of the equipment. Therefore, a method specifically for planar near-field (PNF) measurements is presented in the following, which can be performed in a time- and cost-efficient manner for a large number of AUTs, focusing on array antennas in particular.

The automated alignment procedure is demonstrated using an external laser line profile sensor as described in more detail in Section II. Due to focusing on a planar scan geometry, the sensor can either be permanently mounted alongside the probe antenna on the robot or specifically attached for the calibration process via an automated tool changer. Section III explains the feedback loop to this external measurement device as well as the derivation of the most important metrics related to the AUT alignment including the distance, orientation or its outline, finally allowing to achieve a virtual image of the AUT. Based on this, the geometry of the AUT can be used to ensure the alignment of a user-defined scan plane in relation to the AUT. Furthermore, pre-known reference markings can be detected by the sensor, allowing the system to automatically align the center of the desired scan plane with the geometric center point of the AUT's virtual image. The method is verified using a metal plate whose position can be translated and rotated. Based on the geometric dimensions of this reference object, the method is, therefore, demonstrated for spatially flat antennas or radomes of similar shape. Results for the determined AUT orientation and its outline, both defining the PNF scan plane parameterization, are presented in Section III. Further opportunities based on imaging techniques to optically inspect the AUT are discussed in Section IV.

II. Measurement Setup

The measurement setup consists of a Yaskawa GP-7 robot arm, which is used for experimental test purposes. A Gocator 2430 laser line profile sensor is mounted on its tool flange and its dimension and orientation are defined as a tool in the robot controller. This enables intuitive and efficient operation of the sensor, even if the center of the optics does not coincide with the center of the tool flange or its orientation. Various approaches exist for calibrating the tool, whereby a solution

that is both convenient and suitable for automation is achieved by detecting a reference point for several robot positions. In this case, a calibration tip identified from three robot positions has been used to determine the position of the tool coordinate system. The orientation of the tool coordinate system has been identified by evaluating the height profiles measured with the sensor itself.

A. Laser Line Profile Sensor

An entire product range of laser line profile sensors is available as shown in Fig. 1, whereby a suitable sensor model can be determined for almost any application. The specific sensor model is identified depending on the size of the AUT, the desired measurement distance and the resolution required to identify reference marks or to optically inspect the AUT, respectively.

Figure 1: Examples for laser line profile sensors from LMI Technologies [8].

The results shown in the following have been generated with the Gocator 2430 [9] featuring a height resolution of $6\,\mu\mathrm{m}$ for a measurement range of $80\,\mathrm{mm}$. The clearance distance to the targeted measurement surface is $75\,\mathrm{mm}$ and the field of view variies between $47\,\mathrm{mm} - 85\,\mathrm{mm}$ depending on the actual measurement distance. Raw measurements are processed directly by the sensor yielding a uniform (resampled) sensor output for all measurement distances. Each height profile measured consists of 1500 data points, resulting in a lateral resolution of $37\,\mu\mathrm{m} - 57\,\mu\mathrm{m}$. The measurement rate variies depending on the scan settings between $0.2\,\mathrm{kHz} - 5\,\mathrm{kHz}$, where the results shown has been generated at a measurement frequency of $350\,\mathrm{Hz}$. On the one hand, this ensures a sufficiently high update rate for real-time control of the robot and, on the other hand, prevents unnecessarily large amounts of data from being processed.

The high-precision height resolution of $6\,\mu\mathrm{m}$ ensures that even finest structures of the AUT can be identified, as shown for example in Section IV. However, there are also suitable sensor models for very large AUTs, which, for example, enable a field of view of up to $2\,\mathrm{m}$ with a height resolution of $70\,\mu\mathrm{m}$, thus ensuring accurate imaging results for most applications.

B. Real-Time Control of the Robot

In order to realize planar measurements for unknown AUTs, a real-time interface is used to control the robot-based positioner. In this way, the robot can be operated dynamically and in direct response to the measurement data recorded with the laser sensor. The interface allows, for example, the combination of relative and absolute movements or the creation of new user coordinate frames and many more features. This is advantageous to detect the edges of the unknown AUT or to adapt the desired sampling grids to the AUT's orientation without requiring the use of rigidly programmed motion sequences. Furthermore, this interface facilitates the acquisition of conformal measurements of an AUT that does not have a planar aperture or radome, but may be curved or wave-shaped, while still maintaining a constant measurement distance and correct alignment. Thus, utilizing this next-generation controlling interface provided by Yaskawa enables the highly dynamic, real-time capable, and time-efficient operation of robotic positioners.

III. Alignment Technique

The method relates to the alignment and realization of PNF measurements for spatially flat antennas or radomes of similar shape. For this purpose, it is assumed that the AUT is positioned in an xy-plane of arbitrary orientation. The only prior knowledge required is that the operator of the measurement system positions the robot in any position in z-direction in front of the unknown AUT.

A. Approaching the AUT

Beginning from this arbitrary starting position, the robot approaches the AUT in z-direction until its distance is within the sensor's measurement range. As soon as this is the case, the robot slows down its approaching trajectory until the highest point of the measured profile is in the center of the sensor's measurement range. If the requested PNF measurement distance is supported by the sensor, it can also be approached directly. The only decisive factor is that a sufficient number of data points in the height profile of the laser sensor is available. Thus, for extreme AUT tiltings, it can be advantageous to drive closer to the AUT to ensure a sufficiently large amount of measurements.

B. AUT Orientation

Since a sufficiently large surface of the AUT is now within the measurement range of the laser sensor, the orientation of the AUT can be determined. Therefore, the sensor is rotated around the z-axis of the tool coordinate system, also denoted as rotation R_z, and several height profiles are recorded for a certain angular step size and angular range.

This is illustrated in Fig. 2, which shows the measured height as a function of the lateral measurement position for

several rotations R_z. In addition, a curve f_i determined by linear regression is overlayed which is used to calculate the slope, or the angular tilt α_i for each rotation i, respectively. Thus, the tilt α_i is given by

$$\alpha_i = \sin^{-1}\left(\frac{f_i\left(x_{\text{stop}}\right) - f_i\left(x_{\text{start}}\right)}{x_{\text{stop}} - x_{\text{start}}}\right), \tag{1}$$

where x_{start} and x_{stop} indicate a region in the respective height profile that is as large as possible. Since the angle α_i represents a superposition of the AUT tilts along the x- and y-axis, also referred to as rotations R_x and R_y, the tilts α_i are used to optimize the alignment model given as

$$\begin{pmatrix}\alpha_x\\ \alpha_y\end{pmatrix} = \begin{pmatrix}\beta_x\\ \beta_y\end{pmatrix} + \begin{pmatrix}\sin\left(R_z\right) & \cos\left(R_z\right)\\ -\cos\left(R_z\right) & \sin\left(R_z\right)\end{pmatrix} \cdot \begin{pmatrix}\gamma_x\\ \gamma_y\end{pmatrix}, \tag{2}$$

describing the superposition of different tilts related by the rotation matrix around the z-axis. Thus, solving this nonlinear optimization problem yields static tilts β_x and β_y as well as R_z-depending tilts γ_x and γ_y as has been previously shown for a spherical electrical alignment procedure in [6].

For the same AUT orientation already shown in Fig. 2, the model and the measured support points are compared in Fig. 3 depending on the angle of rotation. It is evident that both data series correspond well to each other. The largest difference occurs at $R_z = 40°$ with a deviation of $0.067°$ between the model and measurement data whereas the average error amounts to only $0.003°$. Therefore, the model provides a very good correlation with the actually measured orientation of the AUT. Due to the high quantity and quality of the measurement data, it is also possible to reduce the angular range for determining the AUT orientation. Therefore, an iterative approach is feasible to evaluate the gradient of the model parameters or the model error compared to the measurements, respectively.

A new user coordinate system is automatically created in the following to simplify handling, also denoted as AUT user frame. The origin of the AUT user frame is determined as described in Section III-A and the orientation takes into account the identified rotations R_x and R_y. As a result, the robot can be moved in a plane parallel to the arbitrarily oriented AUT at a known distance in z-direction.

C. Outline Identification and Orientation

With the determined tilts and the AUT user frame, it is possible to move the laser sensor parallel to the AUT at a known and measureable distance in z-direction. Thus, the first edge of the unknown AUT can be detected starting from the origin of the AUT user frame with a travel direction parallel to the orientation of the measured laser profile. During motion of the robot, the measurement data of the laser sensor is analyzed in real time to detect the first edge of the AUT. If the surface of the AUT is not significantly curved, simple thresholding is sufficient. Once an edge is detected in the measurement range of the laser sensor, the movement speed can be adjusted and reduced using the interface described in Section II-B. Finally, incremental movements are used to precisely position the robot so that the AUT edge is detected in the center of the measured laser profile, which facilitates subsequent data processing.

Once the edge of the AUT is centered in the height profile of the laser sensor, the direction of the edge is determined. Starting from the current position, micro movements in the range of a few millimeters are carried out in both, the x- and y-direction. At the end points of this movements, height profiles are recorded with the laser sensor and the differences in relation to the first position with the centered edge are analyzed. Using trigonometric relationships, the direction of the edge is determined as a first-order approximation. It should be noted that the step width of the micro movements must not be greater than the profile width of the laser sensor, which, however, can easily be ensured for all common laser sensor models.

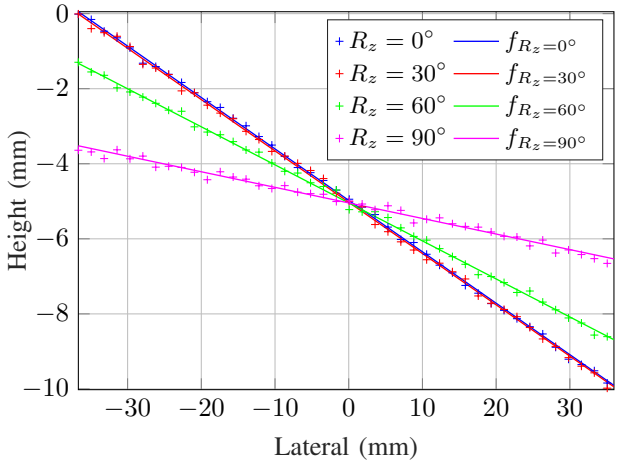

Figure 2: Exemplary height profiles depending on R_z for an AUT orientation of $R_x = -7.5°$ and $R_y = -2°$. The corresponding linear regression f_{R_z} is overlayed.

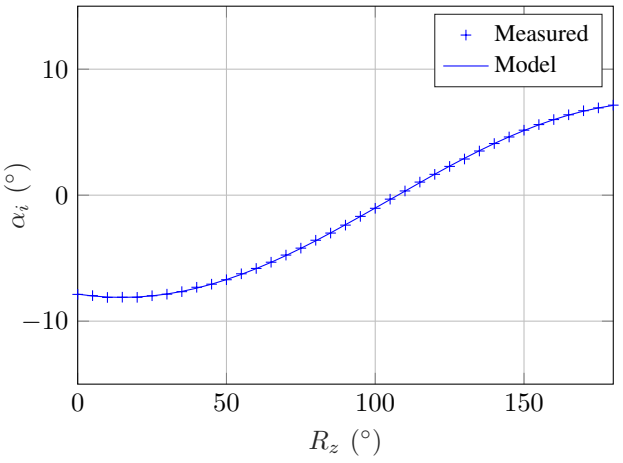

Figure 3: Alignment model compared to the corresponding discrete measurements for the same AUT orientation as shown in Fig. 2.

Finally, the determined orientation of the edge is used to preliminarily realign the R_z-rotation of the robot flange so that the profile of the laser sensor is perpendicular to the edge of the AUT, maximizing the effective field of view during edge tracking as explained hereinafter. Furthermore, the overall AUT outline is used as a second-order estimation of the R_z-rotation for the following measurement steps.

D. Outline Tracking

Once the orientation of the antenna in R_x and R_y has been determined and the position and orientation of the first edge of the AUT has been detected, the entire outline of the AUT is identified. Therefore, the orientation of the edge is used to calculate the scan direction of the robot. In addition, a perpendicular velocity vector is calculated to correct the scanning process in real time. While the robot moves along the scanning direction, the measurement data provided by the laser sensor is continuously evaluated to identify the position of the edge. If the edge is no longer positioned in the center of the height profile, the perpendicular velocity vector is used to correct the robot's scanning direction. Based on the displacement of the identified edge to center of the profile, the perpendicular velocity vector is scaled and, thus, contributes to the position correction process.

If the control loop response is not sufficient to correct the position, i.e. there is a significant change in direction of the edge, or the edge can suddenly no longer be detected, a corner is assumed. Depending on the a priori knowledge available, the sensor head can be rotated by a known angle to continue the edge detection or the edge including its orientation must be detected again. For the latter case, the procedure explained in Section III-C is used again to identify the edge and determine its orientation. Finally, the edge detection process continues to the next corner until the digitization of the entire AUT outline is completed.

The results of the edge detection are shown in Fig. 4. The red circles mark the actual robot position during the scanning process while the measured height of the laser sensor is illustrated color-coded. In addition, the actual sampling rate of the laser sensor is regulated depending on the measurement data obtained. This simplifies the processing of the rather large amounts of data and explains the non-uniformity of the generated point cloud. Measurement data is only recorded with the maximum temporal resolution in areas where reference markings have been identified, which can potentially be used for more precise alignment.

A detailed view of a detected reference mark, in this case a fiducial for determining the alignment, is shown in Fig. 4b. The outline of the hole is clearly visible and therefore, depending on the AUT, such reference marks can be used for alignment as an alternative to the detected AUT outline. In order to avoid acceleration effects of the robot in the area of corners, the reference mark is only identified during movement at the nominal measurement speed and is, thus, only recorded from one side with maximum temporal resolution.

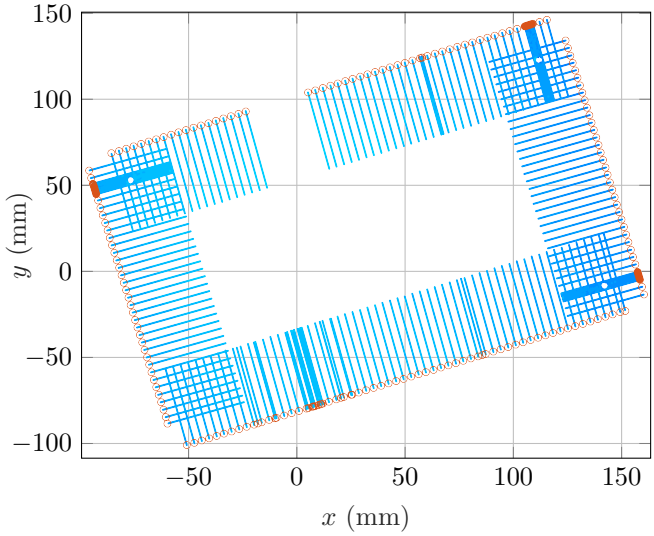

(a) Overview of the AUT's outline identification. The sampling rate is increased in regions where reference markings have been identified as shown in more detail in Fig. 4b.

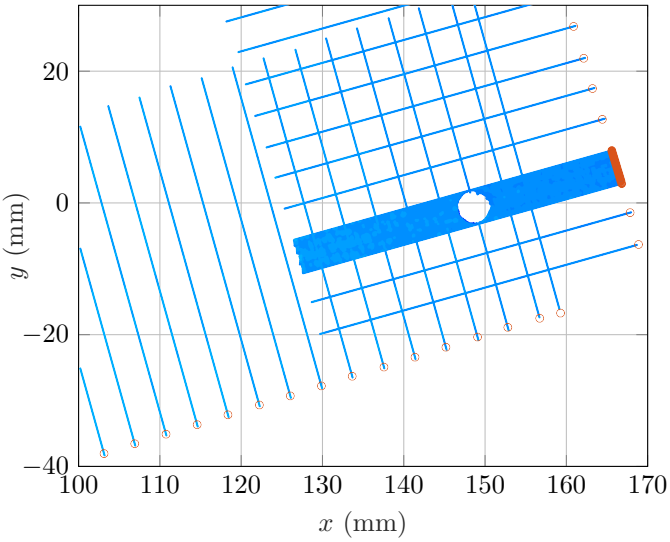

(b) Detailed view on one of the three identified reference markings to visualize the high-resolution imaging capabilities.

Figure 4: Results for tracking of the AUT outline and identification of reference markings. As the color scale is not relevant for edge detection, it is omitted for better visualization.

IV. Imaging Capabilities

In addition to the self-calibration of the measurement setup, the laser sensor can also be used for high-resolution 3D imaging of the AUT, for example to perform an optical inspection. An exemplary image of the test object used is visualized in Fig. 5. The identification of the arbitrarily positioned and oriented AUT has been conducted as explained in Section III. In contrast to the previously shown results, this compensates for all inclinations and offsets, thus resulting in a regular AUT

image which is arranged along the x- and y-axis. All three fiducials that can potentially be used for alignment are clearly visible. It is also evident that the test object has a slightly curved surface, as can be seen from the gradient of the color-coded height measurements.

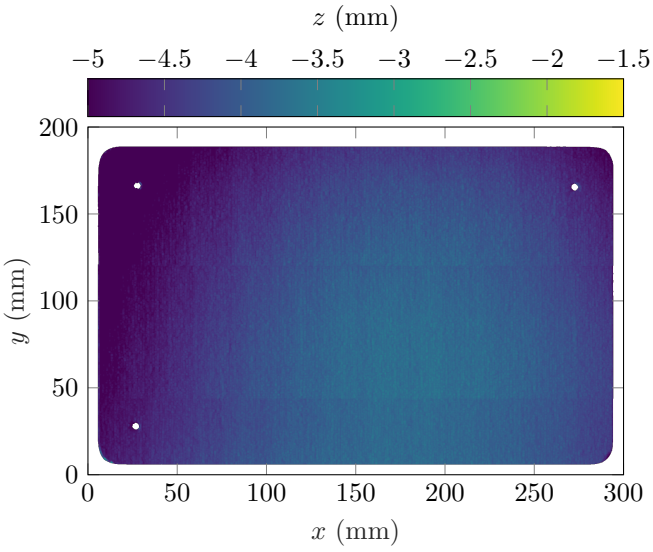

Figure 5: 3D high-resolution image of the AUT for the identified orientation, position and outline using the implemented alignment method.

In a next step, to demonstrate the measurement capabilities, a sheet of paper with the company logo printed on it has been positioned on the test object as illustrated in Fig. 6a. The lettering has been cut out to achieve a more distinct height profile, but not the sinusoidal wave contained in the logo. As even thinnest strips of adhesive tape are visible in the height measurements, further fixing has been omitted. Therefore, the color gradient indicates a slight curvature in the sheet of paper, which can hardly be avoided without additional fixtures. As expected, the letters of the logo are clearly visible. However, a more detailed examination provided in Fig. 6b additionally proves that even the purely printed sine wave is recognizable in the image. It shows a smaller section of the same measurement, but with an adjusted color scale for better visualization. Here, the printed sine wave is clearly visible, which emphasizes that even the thickness of the ink layer from printing can be identified during the optical inspection. Accordingly, smaller cracks, dents or other subtle imperfections in the same order of magnitude can also be detected. This illustrates the potential of an optical inspection, which can be performed directly after the automated calibration process and within the same system, providing a further application for robot-based PNF measurements.

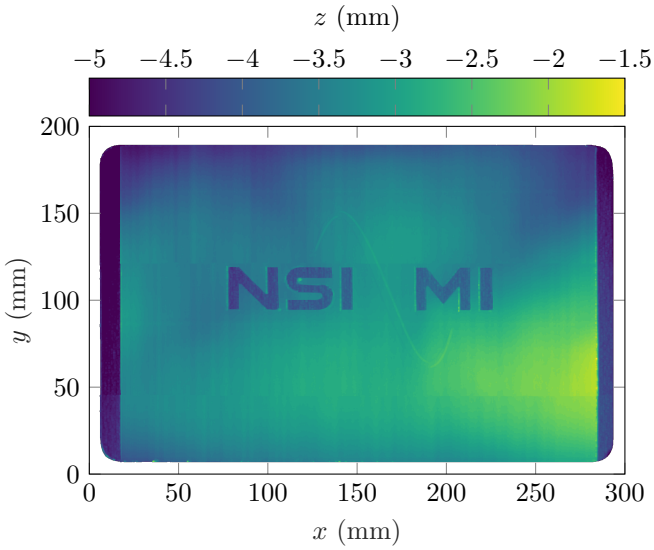

(a) AUT covered by a sheet of paper with the letters of the company logo cut out. The corresponding sine wave pattern has not been cut out, but only printed and is still identified.

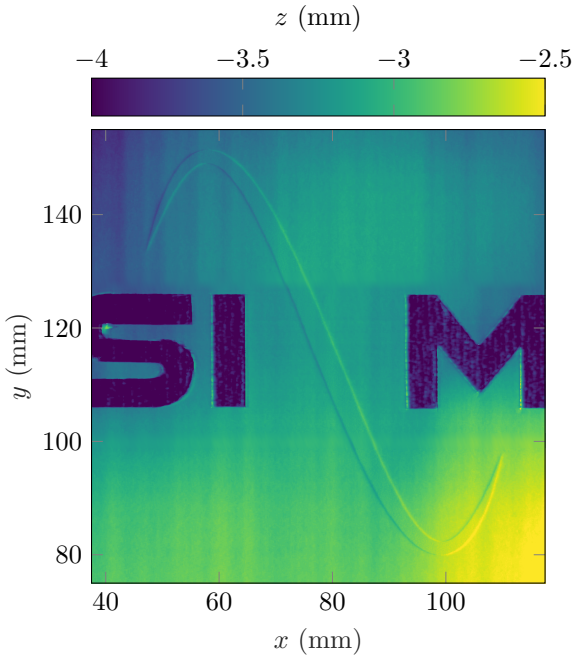

(b) Close-up view with more subtle color scale demonstrating that even the ink layer thickness of the printed sine wave logo is sufficient to be detected by the laser line profile sensor.

Figure 6: Results of 3D imaging of a printed sheet of paper in which only the lettering, but not the sinusoidal wave, has been cut out.

V. Conclusions

The combination of robot-based positioning systems with external sensors opens up numerous new opportunities. For planar applications, laser line profile sensors are suitable for generally flat antennas or radomes. Using real-time capable control interfaces, robots can react dynamically to the shape, position and orientation of the AUT and precisely adapt the calibration sequences. Thus, robot-based measure-

ment systems allow to automatically align the requested sampling geometry to unknown AUTs within minutes. The only prior knowledge required is an arbitrary position in front of the AUT, whereby additional information, for example on the shape of the AUT, can further accelerate the calibration process.

The same sensor and measurement setup can also be used to visually inspect the AUT, thus enabling the detection of surface imperfections such as cracks or dents. Based on the choice of sensor, mostly depending on the size of the AUT, it is even possible to identify a printed layer of ink in the imaging process.

As a result, the combination of robot-based measurements with external sensors allow to operate these systems more flexibly while simultaneously providing new measurement capabilities.

REFERENCES

[1] E. J. Vermeulen and J. Demas, "Robotic near field scanning for high throughput phased array production test," in *18th European Conference on Antennas and Propagation (EuCAP)*, Glasgow, Scotland, Mar. 2024.

[2] S. F. Gregson and C. G. Parini, "Use of compressive sensing techniques for the rapid production test of commercial nose-mounted radomes in a robotic antenna measurement system," in *19th European Conference on Antennas and Propagation (EuCAP)*, Stockholm, Sweden, Mar. 2025.

[3] J. A. Gordon, D. R. Novotny, M. H. Francis, R. C. Wittmann, M. L. Butler, A. E. Curtin, and J. R. Guerrieri, "Millimeter-wave near-field measurements using coordinated robotics," *IEEE Transactions on Antennas and Propagation*, vol. 63, no. 12, pp. 5351–5362, Dec. 2015.

[4] R. Moch and D. Heberling, "Robot-based antenna and radar measurement system at the RWTH Aachen University," in *42nd Antenna Measurement Techniques Association Symposium (AMTA)*, Newport, RI, USA, Nov. 2020.

[5] D. J. van Rensburg, B. Walkenhorst, Q. Ton, and J. Demas, "A robotic near-field antenna test system relying on non-canonical transformation techniques," in *41st Antenna Measurement Techniques Association Symposium (AMTA)*, San Diego, CA, USA, Oct. 2019, pp. 1–5.

[6] H. Jansen, R. Moch, and D. Heberling, "Electrical alignment technique for offset-mounted and arbitrarily oriented AUTs in a robot-based mm-wave antenna test system," in *45th Antenna Measurement Techniques Association Symposium (AMTA)*, Seattle, WA, USA, Oct. 2023.

[7] B. L. Moser and J. Gordon, "Rapid automated antenna alignment on robotic antenna ranges," in *18th European Conference on Antennas and Propagation (EuCAP)*, Glasgow, Scotland, Mar. 2024.

[8] "Gocator 2400 series," https://lmi3d.com/series/gocator-2400-series/, LMI Technologies Inc., last accessed: 2025-06-24.

[9] *Gocator 2400 series data sheet*, LMI Technologies Inc., 2024, revision 1.6 (Last accessed: 2025-06-24). [Online]. Available: https://lmi3d.com/wp-content/uploads/2024/02/DATASHEET_Gocator_2400_US_WEB-1.pdf